Diffraction at HERA
An Experimentalist's View

P. Marage
Université Libre de Bruxelles – CP 230
Boulevard du Triomphe
B-1050 Brussels Belgium
(March 16, 1999)

Diffraction studies at HERA are introduced, with reference to other communications to this Conference. Motivations and specific features of the experimental approaches are stressed.[1]

I. INTRODUCTION

Diffractive scattering of hadrons (see Fig. 1) is closely related to elastic scattering and thus to deepest principles of quantum theory, wave-particle duality and unitarity, through the optical theorem and the Froissard and Pumplin bounds (see e.g. [1,2]).

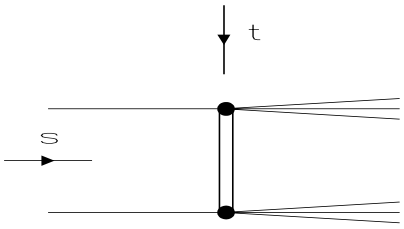

FIG. 1. Diffractive scattering of hadrons, with double diffractive dissociation.

In the s-channel approach, diffractive scattering is explained by the differential absorption by the target of the large number of hadronic states which coherently build up the initial state hadron and scatter with different cross sections [3]. The implied reorganisation in the outgoing system leads to the production of hadron states with different mass and / or quantum numbers, but obeying definite selection rules. Whereas elastic scattering is intimately related to the amount of inelastic scattering (optical theorem) and happens over the full target volume, diffractive scattering is due to fluctuations in the inelastic amplitudes. It is of a peripheral character, since the absorption cross sections for the different hadronic states vary more in the outer ("grey") region of the target than in the center ("black") core. A limitation of the s-channel approach is that it does not provide *ab initio* calculations but requires, for any practical purpose, the use of badly known cross sections and of non-diagonal scattering properties.

In the t-channel approach [1], the scattering properties are related to the characteristics of exchanged virtual particles (with t the squared four-momentum of the exchange), using general properties of unitarity, crossing symmetry and analyticity of the amplitudes. In particular, the energy dependence of the cross section is governed by the spin of the exchanged particles. In a

[1] Paper presented at the LAFEX International School on High Energy Physics, LISHEP 98, Rio de Janeiro, February 1998. The present paper follows closely the content of the talk presented at Rio, with the exception that reference to preliminary results have been updated to published papers where available; a few additions have been included, mainly in the form of footnotes.

generalised form, this leads to the concept of "Regge trajectories": in the t − angular momentum plane, real particles (with squared mass $t > 0$) and virtual states (with $t < 0$) are observed to lie on linear trajectories, characterised by a definite set of quantum numbers and parameterised as

$$\alpha(t) = \alpha(0) + \alpha' \cdot t. \tag{1}$$

For the exchange of a given trajectory, the cross section depends on the centre of mass energy squared s as

$$\sigma \propto s^{\alpha(0)-1}. \tag{2}$$

This approach met tremendous success in the description of total, elastic, single- and double-diffraction scattering cross sections (see e.g. [2,4–6]). In particular, the celebrated Donnachie-Landshoff parameterisation [7] describes the elastic cross section for numerous reactions in terms of the exchange of two main trajectories: the *reggeon* trajectory, related to the ρ meson family, of the form

$$\alpha_{I\!R}(t) \simeq \ 0.55 + 0.9\ t, \tag{3}$$

t being measured in GeV^2, and the *pomeron* trajectory, of the form [2]

$$\alpha_{I\!P}(t) \simeq \ 1.08 + 0.25\ t, \tag{4}$$

which carries the quantum numbers of the vacuum and to which no known particle is associated (except maybe for a glueball candidate [9]). At high energy, elastic and diffractive scattering are dominated by pomeron exchange, which leads to a slow increase of the cross section with s.

In spite of this success, the need of considering multi-reggeon and cut exchange led to intricated mathematics. More fundamentally, questions concerning the nature of the pomeron and the lack of a microscopic theory led in the 70's to *"the death of the Reggeon approach"* [10].

With the advent of QCD as the theory of strong interactions, models were proposed in order to understand diffraction in this framework. In the simplest form, the pomeron was modelised as a two-gluon system [11], and this approach was actively pursued by several authors. At the end of the 80's, the observation by the UA8 experiment of jet production in diffractive $p\bar{p}$ scattering [12] confirmed the assumption by Ingelman and Schlein [13] that the pomeron may be built of partons subjected to hard scattering.

The major discovery of the ZEUS and H1 experiments in deep inelastic scattering (DIS) was the observation in 1992 that the proton structure function $F_2(Q^2, x)$ is sharply rising for small x values (i.e. high energy). This "hard" behaviour, observed even for low Q^2 values [14,15] contrasts with the "soft" behaviour of high-energy hadron−hadron cross sections (eq. 4).

A second major result was the *"Observation of Events with a Large Rapidity Gap in Deep Inelastic Scattering at HERA"* by ZEUS using a sample of $\simeq 25$ nb^{-1} accumulated in 1992 [16], confirmed by H1 with 300 nb^{-1} of data taken in 1993 [17]. These large rapidity gap (LRG) events, attributed to diffraction, were observed to make a contribution to the DIS cross section at a level of 8−10%, with a leading twist Q^2 dependence. They are characterised (see an example in Fig. 2) by the absence of activity in the "forward" part of the detectors.[3] In contrast, for non-diffractive "usual" DIS events, a colour string extends through the forward region, connecting the proton remnant and the struck quark, which leads to particle emission.

It is true to say [18] that this observation was a surprise for many experimentalists: few papers dealing with diffraction in DIS were presented at the 1987 and 1991 Workshops on HERA physics

---

[2] An analysis by Cudell et al. [8] gives for the pomeron intercept a preferred value $\alpha_{I\!P}(0) \simeq 1.10$, with extreme acceptable values of 1.07 and 1.11.

[3] In the HERA convention, the "forward" ($+z$) direction is that of the outgoing proton beam; unless stated otherwise, the transverse direction is defined here with respect to the beam direction.

[19], no diffractive Monte Carlo in DIS was available, and the detectors were not well equipped for diffractive studies (nor for low-x physics in general). It was also true to state, as written in the first experimental HERA paper on diffraction, that "until recently, Regge theory and perturbative QCD have been subjects without much overlap" [16].

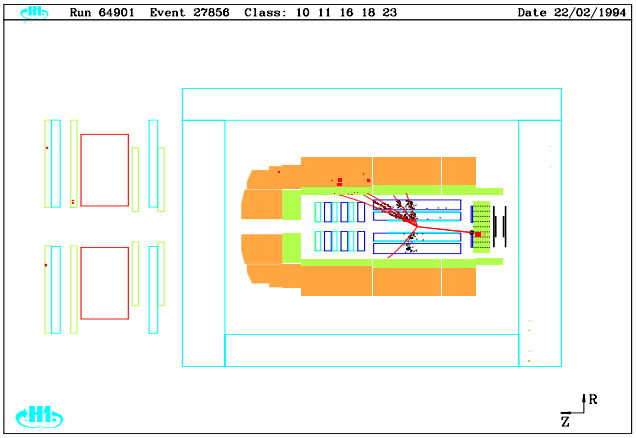

FIG. 2. A typical diffractive DIS event in the H1 detector. The electron is scattered on the right, in the backward electromagnetic calorimeter. No activity is detected in the forward part of the liquid argon calorimeter nor in the forward detectors, in particular the forward muon detectors, on the left.

In the last few years, however, considerable progress have been made in both experimental and theoretical research, as testified by the large number of published papers and of workshops devoted to diffraction. In addition to HERA, diffraction has been intensively studied at the Fermilab Tevatron [20]. Interactions between experimentalists and theorists have intensively developed, the complexity of the subject making the guidance of experiment important for the progress of theory.

II. INCLUSIVE MEASUREMENTS OF THE DIFFRACTIVE CROSS SECTION

Huge efforts have been invested by the experimental collaborations to achieve a precise measurement of the inclusive diffraction cross section at HERA. Common definitions of the relevant variables have been accepted, the concept of "diffractive structure functions" has emerged as a useful tool and, most important, experimental procedures and their inter-relations have been discussed and clarified (in particular the question of non-diffractive background subtractions), in order to define precisely and unambiguously the object of the studies.

A. Kinematics; Diffractive Structure Functions

Diffractive ep interactions are sketched in Fig. 3. The characteristic feature is that the final state hadronic system, with centre of mass energy W,[4] is divided into two subsystems of

[4]Here, the mass W is always supposed *large*, i.e. $W \gg M_p$, M_p being the proton mass. Note that the centre of mass hadronic energy is called W in deep-inelastic scattering and $\sqrt{s}$ for hadron–hadron interactions; in DIS, $\sqrt{s}$ is the $e-p$ centre of mass energy.

significantly lower mass, separated by a large gap in rapidity: the system X, of mass M_X, which corresponds to photon dissociation, and the system Y, of mass M_Y, which consists in a proton or an excited baryonic state, with small transverse momentum $p_T \simeq \sqrt{|t|}$. An important feature is that the size of the gap in rapidity is significantly larger than implied by particle density fluctuation during the hadronisation process for non-diffractive interactions, and is thus attributed to the exchange of a colour-singlet system, specifically reggeon or pomeron.[5]

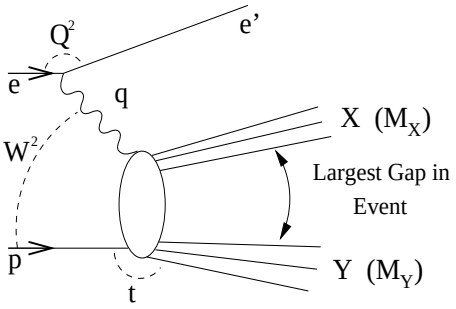

FIG. 3. Deep-inelastic diffractive interaction.

In the particular case where the proton remains intact, the diffractive process

$$e + p \to e + X + p \tag{5}$$

is defined, up to an azimuthal angle between the electron and the proton scattering planes, by four kinematical variables. These are conveniently chosen as Q^2, $x_{I\!P}$, β and t, where Q^2 is the negative of the squared four-momentum of the photon, t is the squared four-momentum transfer to the proton, and $x_{I\!P}$ and β are defined as

$$x_{I\!P} = 1 - x_L \simeq \frac{Q^2 + M_X^2}{Q^2 + W^2} \tag{6}$$

$$\beta \simeq \frac{Q^2}{Q^2 + M_X^2}, \tag{7}$$

x_L being the fraction of the incident proton energy carried by the scattered proton.

The variable $x_{I\!P}$ can be interpreted, in the proton infinite momentum frame, as the fraction of the proton momentum carried by the exchange (reggeon or pomeron) and β is the fraction of the exchanged momentum carried by the quark struck by the photon. These variables are related to the x scaling variable (with $W^2 \simeq Q^2/x - Q^2$) by the relation

$$x = \beta \cdot x_{I\!P}. \tag{8}$$

Kinematics imply that, at high energy, a large gap in rapidity is created between the system X and the scattered proton when $x_{I\!P} \ll 1$, i.e. $M_X \ll W$.

In analogy with non-diffractive DIS scattering, the measured cross section is expressed in the form of a four-fold *diffractive structure function* $F_2^{D(4)}(Q^2, x_{I\!P}, \beta, t)$:

$$\frac{\mathrm{d}^4\sigma\ (e + p \to e + X + p)}{\mathrm{d}Q^2\ \mathrm{d}x_{I\!P}\ \mathrm{d}\beta\ \mathrm{d}t} = \frac{4\pi\alpha^2}{\beta Q^4}\ (1 - y + \frac{y^2}{2(1 + R_D)})\ F_2^{D(4)}(Q^2, x_{I\!P}, \beta, t), \tag{9}$$

[5] As will be mentioned below (section IIIB), approaches have also been proposed for LRG event production which do not refer to diffraction as a specific process, but are based on colour reorganisation through soft processes.

where y is the usual scaling variable, with $y \simeq W^2/s$, and R_D is the ratio of the longitudinal and transverse diffractive cross sections. R_D has not been measured so far.[6] Its value is commonly put to 0 for extracting the diffractive structure function, which has a small impact on the measurements performed in the presently accessible y range.

Experimentally, the t variable is usually not measured or is integrated over. Results are thus mostly presented for the three-fold diffractive structure function $F_2^{D(3)}(Q^2, x_{I\!P}, \beta)$. The latter is conveniently parameterised in the *factorised* form

$$F_2^{D(3)}(Q^2, x_{I\!P}, \beta) = \Phi(x_{I\!P}) \cdot F_2^D(Q^2, \beta), \tag{10}$$

with a Regge inspired parameterisation:

$$\Phi(x_{I\!P}) \propto x_{I\!P}^n \tag{11}$$

and

$$n = 2 \cdot \langle \alpha(t) \rangle - 1. \tag{12}$$

For pomeron exchange, and if factorisation holds, the factor $\Phi(x_{I\!P})$ can be interpreted as describing an effective pomeron flux in the proton, whereas the function $F_2^D(Q^2, \beta)$ describes the pomeron structure, β playing the role of x for hadron structure functions.

Several methods are used to extract the diffractive (i.e. pomeron exchange)[7] cross section from the deep-inelastic data. The challenge for experimentalists is to measure a well-defined quantity, not depending on models for background subtraction, and to minimise the contamination of non-diffractive events and of diffractive events with proton dissociation.

B. Rapidity Gap Measurement Method; Reggeon Contribution

A natural way to study diffraction experimentally is to select events with a large rapidity gap, since the latter is kinematically related to small values of $x_{I\!P}$ and thus, at high energy, to pomeron exchange.

This procedure is used by the H1 experiment, which takes advantage of a good coverture of the forward region. Specifically, events are selected, for which hadronic activity is observed in the central detectors, whereas the pseudorapidity [8] of the most forward track or energy deposit in the central calorimeter is $\eta_{max} = 3.2$ and no activity is registered in the "forward detectors", i.e. the "plug" calorimeter, the forward muon detectors and the proton remnant tagger. These detectors overlap in acceptance and are sensitive to primary particles emitted at small angle and to secondaries due to rescatterings in the beam pipe wall or adjacent collimators. For these events, no hadron emission is thus observed in the large rapidity region $3.2 < \eta < 7.5$. The selected sample is consequently restricted to events with an elastically scattered proton or a low mass ($M_Y \lesssim 1.6$ GeV) proton dissociation system (the latter contribute a few % of the selected events), with $|t| \lesssim 1$ GeV^2.

The ZEUS experiment has similarly selected, in the 1993 data sample, events with $\eta_{max} = 2.5$, using only the main calorimeter. The implied relatively small gap in rapidity (the calorimeter extends up to $\eta \simeq 3.8$) required the use of Monte Carlo simulations to estimate the contamination of non-diffractive events with a gap due to particle density fluctuation during hadronisation and of events with proton dissociation.

[6] The measurement of R_D would be of great interest, since various models make different predictions for the longitudinal cross section (see the review [23]).

[7] The term diffraction is often used, in a wide sense, for events with a large rapidity gap; strictly speaking, it applies to pomeron exchange.

[8] The pseudorapidity η of a detected object is defined as $\eta = -\log \tan(\theta/2)$, θ being the emission angle defined with respect to the outgoing proton beam direction.

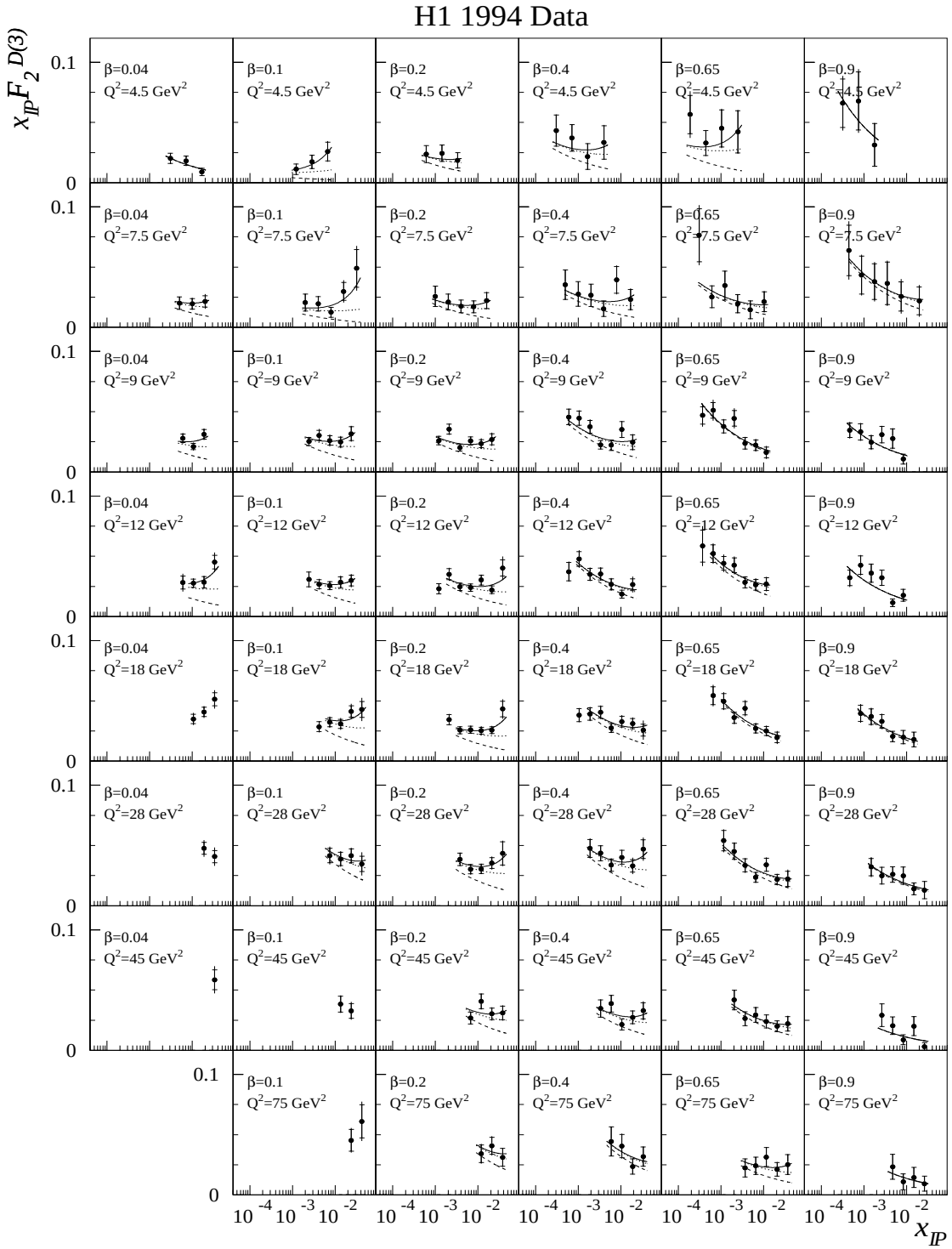

FIG. 4. H1 measurement of $x_{I\!P} \cdot F_2^{D(3)}(Q^2, x_{I\!P}, \beta)$ ($M_Y < 1.6$ GeV, $|t| < 1$ GeV^2) as a function of $x_{I\!P}$ for various Q^2 and β values, with the 1994 data. The curves show the results of the Regge fit with interference. The dashed curves show the contributions from the pomeron alone, the dotted curves, the pomeron plus interference, and the continuous curves, the total.

With the integrated luminosity of $300 - 500$ nb^{-1} accumulated in 1993, the H1 and ZEUS experiments could present a first measurement of the diffractive structure function $F_2^{D(3)}$ as a function of $x_{I\!P}$, for different bins in Q^2 and β [21,24]. Within the measurement precision, factorisation in the sense of eqs. 10 and 11 was observed.

The integrated luminosity of 2 pb^{-1} accumulated in 1994 by the H1 experiment allowed the measurement of $F_2^{D(3)}$ in a total of 47 bins in β and Q^2 ($0.04 < \beta < 0.9$ and $4.5 < Q^2 < 75$ GeV^2) with $x_{I\!P} < 0.05$, the kinematically accessible $x_{I\!P}$ range varying from bin to bin (see Fig. 4) [25]. This measurement has been extended by H1 to low Q^2 values ($0.4 < Q^2 < 5$ GeV^2) using the 1995 data with a vertex shifted towards the forward direction in the detector, and to $200 < Q^2 < 800$ GeV^2, using the statistics accumulated in $1995 - 1997$ [26].

With the increased precision of these measurements, presented in the sensitive form of the $x_{I\!P} \cdot F_2^{D(3)}$ distribution, the apparent factorisation of eq. 10 was broken. This feature was explained as due to the superposition of two contributions, corresponding respectively to pomeron and reggeon exchange:

$$\begin{aligned} F_2^{D(3)}\,(Q^2, x_{I\!P}, \beta) &= \Phi^{I\!P}(x_{I\!P}) \cdot F_2^{I\!P}(Q^2, \beta) + \Phi^{I\!R}(x_{I\!P}) \cdot F_2^{I\!R}(Q^2, \beta) + \text{interf.} \\ &= x_{I\!P}^{2\cdot\langle\alpha_{I\!P}\rangle - 1} \cdot F_2^{I\!P}(Q^2, \beta) + x_{I\!P}^{2\cdot\langle\alpha_{I\!R}\rangle - 1} \cdot F_2^{I\!R}(Q^2, \beta) + \text{interf.} \end{aligned} \tag{13}$$

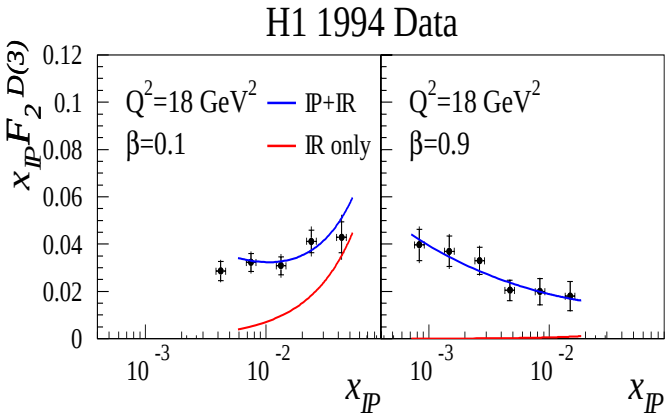

FIG. 5. H1 measurement of $x_{I\!P} \cdot F_2^{D(3)}(Q^2, x_{I\!P}, \beta)$ as a function of $x_{I\!P}$ for two Q^2 and β values, with the 1994 data. The lower curves correspond to the reggeon contribution only, the upper curves to the summed reggeon and pomeron contributions.

From a Regge fit of the data to eq. 13, the reggeon trajectory intercept is found to be $\alpha_{I\!R}(0) = 0.50 \pm 0.18$, in agreement with the expected value (eq. 3), and the pomeron intercept is measured to be $\alpha_{I\!P}(0) = 1.20 \pm 0.04$, higher than for soft interactions (see discussion in section II E). In the case of an incoming virtual state, the strength of the interference between pomeron and reggeon exchange is not known [27]; the data are compatible with maximum as well as with no interference [25].

The detailed contributions of pomeron and reggeon exchange are illustrated on Fig. 5. The reggeon contribution is larger for larger values of $x_{I\!P}$, which correspond to smaller energy (for given Q^2 and β values, $x_{I\!P} = x/\beta \simeq Q^2/[\beta \cdot W^2]$). It is also larger for small values of β, which is consistent with the expected decrease with β of the reggeon structure function, following the meson example, whereas the pomeron structure function is observed to be approximately flat in β (see Fig. 12 below).

Within the precision of the measurement, no evidence is found for factorisation breaking of the pomeron term itself, also when the lower Q^2 data are included [26].

C. The $\ln M_X^2$ Measurement Method

The ZEUS experiment [28–30] has also exploited the fact that diffractive interactions are characterised by a non-exponentially suppressed rapidity gap.

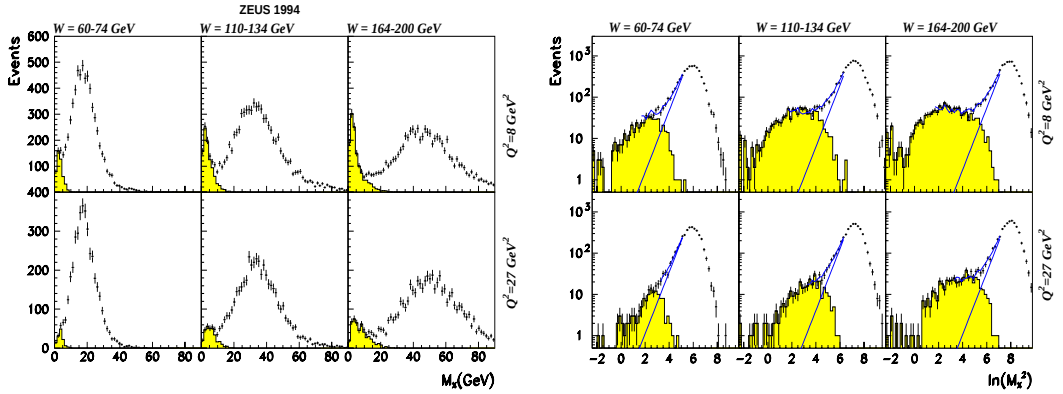

FIG. 6. Distribution of M_X (left) and $\ln M_X^2$ (right) for the ZEUS 1994 data. The shaded histograms show the distribution of events with $\eta_{max} < 1.5$. The straight lines in the right-hand side figures give the non-diffractive contributions as obtained from an exponential fit to the data.

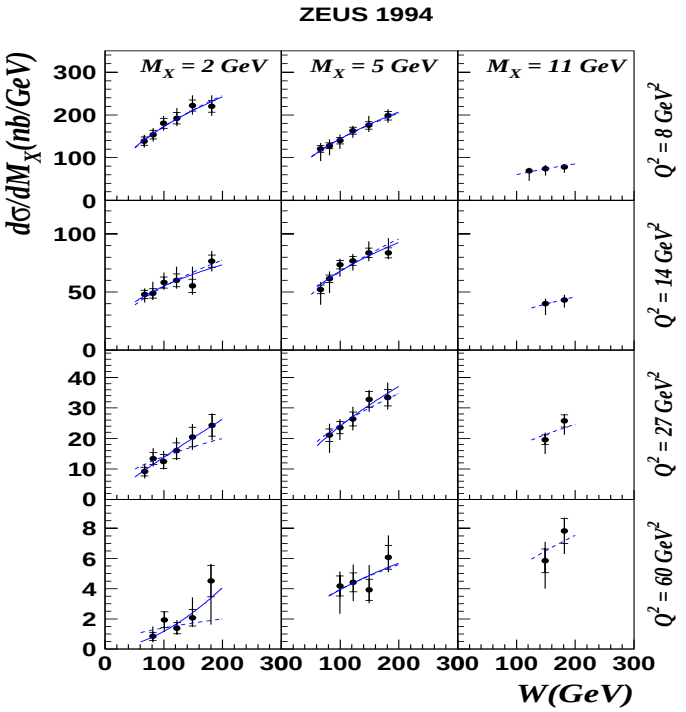

FIG. 7. ZEUS measurement of the differential cross section $d\sigma^{diff}_{\gamma^* p \to XY}/dM_X$ with $M_Y < 5.5$ GeV as a function of W for several M_X and Q^2 values. The solide curves show the result of fitting the diffractive cross section for each (W, Q^2) bin separately as a power of W; the dashed curves show the result of the fit when the power of W is assumed to be the same for all bins.

For fixed values of the hadronic centre of mass energy W, this feature of diffraction corresponds to a non-exponentially suppressed contribution to the M_X mass distribution at amall M_X, as

reconstructed in the central detector.[9] The diffractive contribution is observed in Fig. 6 for small values of M_X, whereas for large M_X the distribution can be parameterised as a single exponential (the falling flange at largest M_X values is due to detector acceptance).

The diffractive cross section is thus extracted for several Q^2 and W intervals (see Fig. 7), after subtraction of the exponentially falling non-diffractive background. The ZEUS detector acceptance implies that events are selected with $M_Y < 5.5$ GeV. For the selected (M_X, W, Q^2) bins, $x_{I\!P}$ is effectively kept below 0.01, leading to a negligible contribution of reggeon exchange.

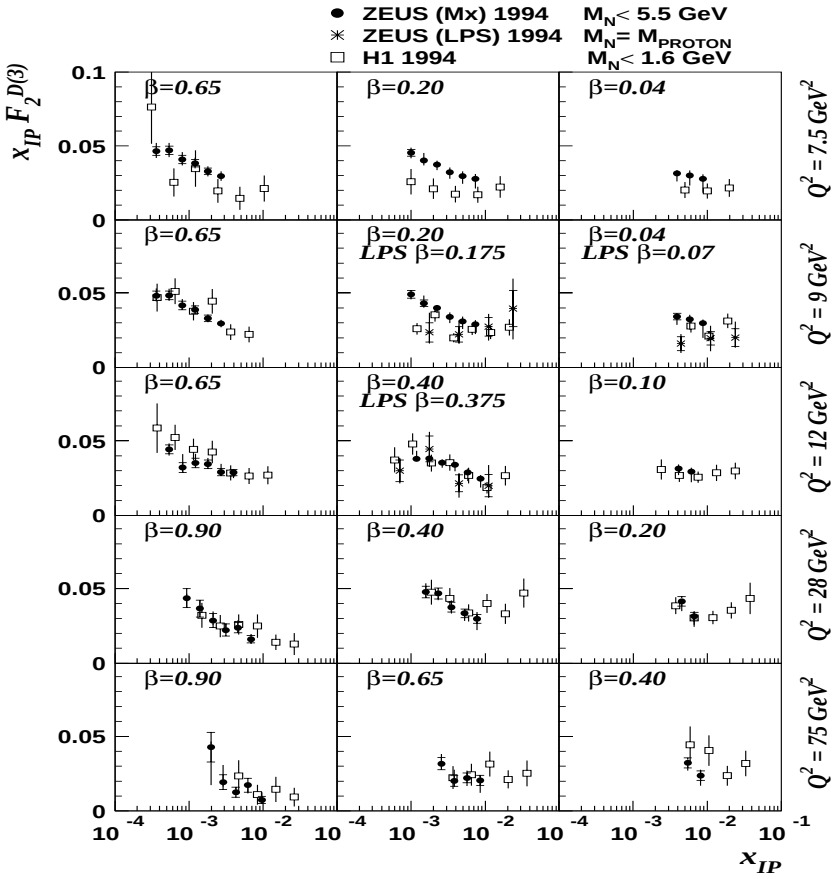

FIG. 8. Measurement of $x_{I\!P} \cdot F_2^{D(3)}(Q^2, x_{I\!P}, \beta)$ as a function of $x_{I\!P}$ for various Q^2 and β values with the 1994 data: ZEUS LPS data (stars), ZEUS data with the $\ln M_X^2$ method (solid points), and a subsample of the H1 measurements (open squares).

D. LPS Measurement; the t Slope

Finally, the ZEUS collaboration has also measured the diffractive structure function, using their leading proton spectrometer (LPS) [31].

The use of proton spectrometers, which detect protons with energy close to the beam energy, provides a clean measurement of the diffractive cross section since the scattered proton is

[9] The pseudorapidity gap $\Delta\eta$ is related to $\ln M_X$ by the relation $\Delta\eta \approx \ln (W^2/M_X^2)$.

unambiguously tagged, avoiding contaminations due to proton dissociation events and to particle density fluctuations in the central detector. Another advantage of the LPS is that the proton momentum measurement leads to a direct determination of $x_{I\!P}$ (see eq. 6). However, the drawbacks of the present ZEUS and H1 proton spectrometers are the limited statistics (the acceptance is $5-7\%$) and the limited range in t ($0.1 \lesssim |t| \lesssim 0.4$ GeV^2 for $x_{I\!P} < 0.03$), which implies that the cross section estimate requires an extrapolation in t of the measurement.

The diffractive structure function measured by ZEUS with the LPS is presented in Fig. 8, together with the ZEUS $\ln M_X^2$ and a subsample of the H1 measurements. Given the large errors, the LPS measurement is in agreement with the other results.

Proton spectrometers have also the unique ability of providing a measurement of the t distribution for inclusive events. The ZEUS LPS has been used to measure the t distribution both in photo- and electroproduction [31–33]. For $3 < Q^2 < 150$ GeV^2, $x_{I\!P} < 0.03$, $60 < W < 270$ GeV, $M_X > 2$ GeV and $0.073 < |t| < 0.40$ GeV^2, the t distribution has been measured with the ZEUS LPS to be exponential, with a slope

$$b = 7.1 \pm 1.0\ (\text{stat.}) \pm 1.2\ (\text{syst.})\ \text{GeV}^{-2}. \tag{14}$$

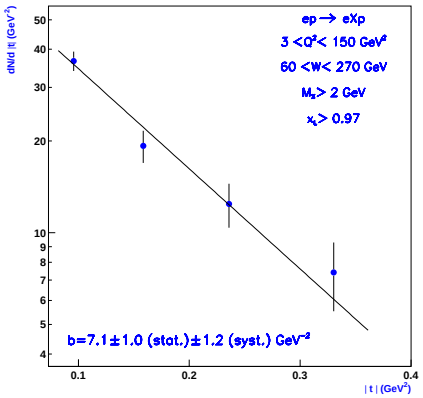

FIG. 9. Differential t distribution of diffractive interactions with $3 < Q^2 < 150$ GeV^2, $x_{I\!P} < 0.03$, $60 < W < 270$ GeV and $M_X > 2$, as measured by the ZEUS collaboration using the Leading Proton Spectrometer.

No Q^2 dependence of the slope is observed in the electroproduction data. A photoproduction measurement gives a very similar value [32]. This has to be contrasted with the strong dependence with Q^2 of the ρ meson production slope.

E. "Soft" and "Hard" Inclusive Diffraction

Although "soft" diffraction may be only an "effective" concept, it will be used here as referring to a mild energy dependence in the parameterisation of eq. 2, typical of hadron−hadron scattering at high energy (cf. eq. 4), in contrast with the stronger energy dependence characterised by a pomeron intercept of the order of $1.2 - 1.3$, as observed in inclusive DIS [14,15] and in diffractive J/ψ production [34,35].

In photoproduction, measurements of the inclusive diffractive cross section have been performed by the H1 [36] and ZEUS [37] experiments. In both cases, the energy dependence was found to be consistent with "soft" diffraction. A triple-Regge analysis was performed of the W and M_X dependences of the H1 data, complemented with lower energy data. While this analysis indicates the presence of a sizeable non-diffractive contribution, the fitted pomeron intercept is

$$\alpha_{I\!P}(0) = 1.07 \pm 0.05. \tag{15}$$

The description of the ZEUS data in the range $8 < M_X < 24$ GeV with a purely triple-pomeron diagram gives for the pomeron intercept

$$\alpha_{I\!P}(0) = 1.12 \pm 0.09; \tag{16}$$

a substantial non-diffractive contribution is found to be necessary at low mass.

In contrast, in DIS diffractive scattering, the pomeron intercept $\alpha_{I\!P}(0)$ is inconsistent with a "soft" value (see Fig. 10). The H1 measurement is

$$\alpha_{I\!P}(0) = 1.20 \pm 0.02\ (\text{stat.}) \pm 0.01\ (\text{syst.}) \pm 0.03\ (\text{model}), \tag{17}$$

with no significant β or Q^2 dependence over the range $0.4 < Q^2 < 75$ GeV^2 [25,26]. The ZEUS measurements are similar, also with no significant Q^2 dependence over the measured range [29,30] (see Fig. 10). Both measurements lie significantly above the "soft" pomeron values, although they seem to be below the "hard" values measured in inclusive DIS. This suggests that inclusive diffraction may be putting the stage for interplay between soft and hard processes.

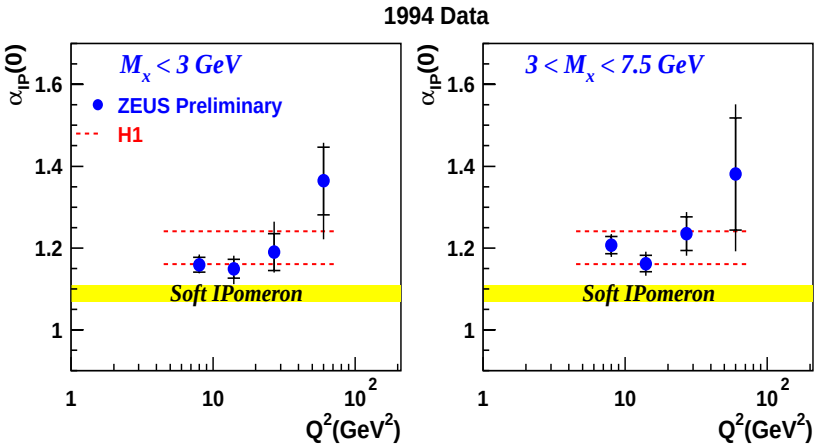

FIG. 10. Measurement of $\alpha_{I\!P}(0)$ for H1 (the measurement limits are indicated as the dotted lines) and for ZEUS (dots).

III. PARTONIC STRUCTURE OF DIFFRACTION

Given the fundamental aspect of diffraction in hadron−hadron interactions, its understanding in terms of partons is a major challenge for QCD. This understanding is helped by the use of two complementary pictures: photon hadronic fluctuations and pomeron structure function. The parton densities in the pomeron extracted from the study of scaling violations can then be extended, under the assumption of factorisation, to the study of inclusive final states and semi-inclusive processes.

A. Two Complementary Pictures

In a traditional approach of diffraction, LRG events are attributed to the exchange in the t-channel of a colourless object, the pomeron, which is sensitive to hard interactions, is flavour blind and carries the quantum numbers $J^{PC}I^G = 0^{++}0^+$ of the vacuum. In this context, diffractive interactions can be conveniently visualised in two different Lorentz frames.

In the *proton rest frame* (see Fig. 11a,c), or any fast moving frame with respect to the photon, relativistic time dilatation implies that photon fluctuations into hadronic systems ($q\bar{q}$,

$q\bar{q}g$, etc.), taking place at a long distance from the proton, appear as "frozen" during the (much shorter) interaction time with the proton. In this approach, the diffractive cross section is thus calculated as the convolution of three factors, corresponding respectively to the (long-lived) photon hadronic structure, the (short time) diffractive interaction between the photon hadronic components and the proton, and the (long-time) hadronisation and final state parton recombination:

$$\sigma_D(\gamma + p \to X + Y) = \sum_{q\bar{q}, q\bar{q}g, \ldots} \int \mathrm{d}^2 b_T \; \Psi(\gamma \to q\bar{q}, \ldots) \cdot \sigma(q\bar{q}, \ldots + p \to q\bar{q}, \ldots + p) \cdot \Psi(q\bar{q}, \ldots \to h). \tag{18}$$

These calculations are usually performed in the impact parameter space (b_T), and only the first Fock states ($q\bar{q}$, $q\bar{q}g$) are considered. The pomeron is parameterised as a two gluon sytem or a Lipatov ladder, which meets the requirements of colour neutrality and flavour blindness.

The *pomeron structure function* approach is developed in the pomeron (or proton) infinite momentum frame, and views the pomeron as a colour singlet partonic object emitted from the proton. In this approach, if the concept of flux factorisation *à la* Ingelman-Schlein [13] holds, the virtual photon probes the pomeron structure similarly to the probing of the proton structure by the photon in "normal" DIS.[10] The DGLAP equations may then describe the QCD evolution of the pomeron structure function (see however below, section III C).

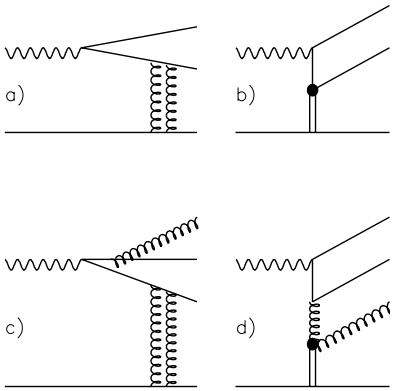

FIG. 11. Photon-proton diffractive interaction: a,c) visualised in a frame moving fast with respect to the photon: the photon fluctuates in a $q\bar{q}$ (a) or a $q\bar{q}g$ Fock state (c), wich subsequently diffractively scatters on the proton (here, the pomeron is modelised as a two-gluon system, and only one of the relevant diagrams is shown); b,d) visualised in the Breit frame, the pomeron being parameterised as a $q\bar{q}$ system, with direct photon−quark coupling (b), or as a gg system, with photon-gluon fusion (d).

These two complementary pictures of diffraction have of course to be consistent with each other. In a semiclassical approach, they have been shown to be equivalent in the case of soft gluon emission off the photon (a $q\bar{q}$+ soft g Fock state) [41].

B. Alternative Approaches

In recent years, models have been proposed to explain the production of LRG events in excess over expectations for particle fluctuation, without reference to the specific concepts of diffraction

[10] Although factorisation is not expected to hold when transporting parton distributions extracted in DIS diffraction to the case of hadron−hadron interactions or of interactions with a resolved photon [38,39], it was shown to hold for diffractive DIS and direct photoproduction [40].

or pomeron exchange. Here, the formation of LRG events is seen as a two-step process. The first step is similar to "normal" DIS events, a quark being ejectecd off the proton by the photon. In a second stage, soft colour interactions (SCI) modify the colour properties of the outgoing system, leading to the formation of two colour-neutral systems separated by a gap in rapidity.

In a semi-classical approach [42], the propagation of the struck parton through the proton colour field is accompanied by soft colour rotation which leads, for a fraction of the events, to colour neutralisation.

The concept of SCI has also been implemented into the LEPTO Monte Carlo calculation [43] where, before hadronisation, parton reconnection takes place through the exchange of soft gluons, leading to the formation of colour neutral systems.

C. Parton Distributions in the Pomeron

Fig. 12 presents the 1994 H1 measurement of $x_{I\!P} \cdot F_2^{D(3)}(Q^2, x_{I\!P}, \beta)$ interpolated to $x_{I\!P} = 0.003$,[11] as a function of β for several Q^2 values. In strong contrast to the hadron structure function at high x, the pomeron structure function is large for high β values, even for relatively large Q^2. In Fig. 13, the H1 measurement is shown as a function of Q^2 for several β values. Scaling violations with a positive slope are observed up to large β values, which suggests that the pomeron is dominated by hard gluons.

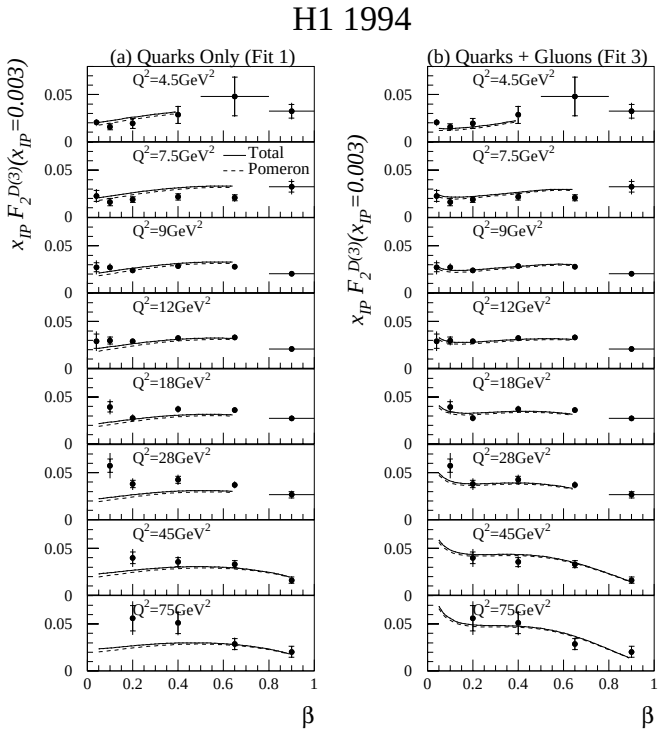

FIG. 12. H1 measurement (1994 data) of $x_{I\!P} \cdot F_2^{D(3)}(Q^2, x_{I\!P}, \beta)$ interpolated to $x_{I\!P} = 0.003$, as a function of β for several Q^2 values. The superimposed curves represent a) a DGLAP fit with quarks only at the starting scale $Q_0^2 = 3$ GeV^2; b) the preferred QCD fit with quarks and gluons at the starting scale.

[11] At this low $x_{I\!P}$ value, the reggeon contribution to $F_2^{D(3)}$ is negligible.

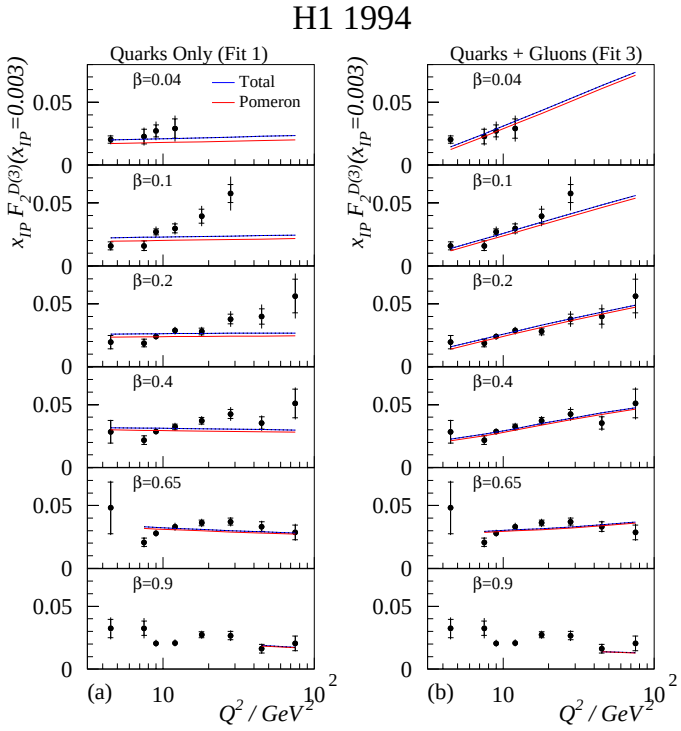

FIG. 13. H1 measurement (1994 data) of $x_{I\!P} \cdot F_2^{D(3)}(Q^2, x_{I\!P}, \beta)$ interpolated to $x_{I\!P} = 0.003$, as a function of Q^2 for several β values. The superimposed curves represent a) a DGLAP fit with quarks only at the starting scale $Q_0^2 = 3$ GeV^2; b) the preferred QCD fit with quarks and gluons at the starting scale.

To analyse quantitatively the pomeron structure, DGLAP fits to the 1994 diffractive structure function presented in Fig. 4 have been performed by H1 for the two contributions of eq. 13, thus assuming factorisation [25].[12] The reggeon contribution is parameterised using the pion structure function [44], and two cases are considered for the pomeron structure function. In the first case, only quarks are allowed to contribute at the starting scale $Q_0^2 = 3$ GeV^2 ("fit 1" in [25]); this gives a poor χ^2: 314 for 159 d.o.f. – see the curves superimposed on Figs. 12a, 13a. In the second case, gluons are also allowed to contribute at the starting scale, and a good description of the data is obtained: χ^2/d.o.f. $= 176/154$ – see the curves on Figs. 12b, 13b.

From this DGLAP analysis, parton distributions are extracted. The distributions corresponding to the best fit to the H1 data ("fit 3" in [25]) are presented in Fig. 14 as a function of z, the pomeron momentum fraction carried by the parton entering the hard interaction (note that $\beta = z$ for quarks but $\beta \leq z$ for gluons). This distribution shows an enhancement of the gluon contribution at high z for small Q^2 values (the turn-over at high z was forced into the fit in order to avoid a singular behaviour of the gluon distribution). A nearly equally good fit ("fit 2" in [25]), also presented in Fig. 14, is obtained with a gluon distribution flat in z at the starting scale. In both cases, the gluons amount to $\geq 80\%$ of the pomeron partonic content in the present Q^2 range, and the parton distribution functions are dominated by hard gluons.

Similar studies were performed by the ZEUS collaboration [45] (see also [46]). In this case, simultaneous fits were performed to the $F_2^{D(3)}(Q^2, x_{I\!P}, \beta)$ distributions in DIS and to the jet diffractive photoprodution cross section. These analyses also lead to the conclusion that gluons

[12] Including the 1995 shifted vertex low Q^2 data does not change the results of the analysis [26].

dominate the pomeron structure: at a scale of 4 GeV^2, the ZEUS analysis indicates that the fraction of the pomeron momentum carried by gluons lies between 0.64 and 0.94. Note however that in such a simultaneous fit, possible factorisation breaking effects (e.g. related to secondary interactions of photon remnants with the proton in the resolved regime of photoproduction) are not taken into account, nor a possibly different interplay between "hard" and "soft" diffraction for the two processes.

From an empirical point of view, a major merit of these DGLAP analyses is that they provide good fits to the data, based on simple assumptions, and that the results can easily be implemented in Monte Carlo simulations in order to test in various semi-inclusive analyses, the universality of the extracted parton distributions.

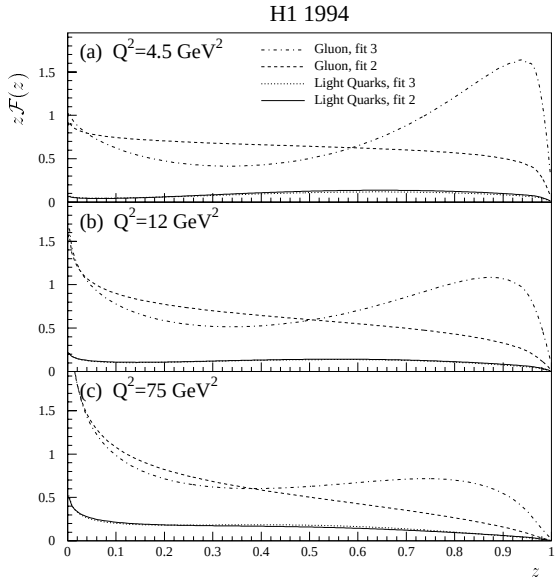

FIG. 14. Parton distributions for three Q^2 values, as obtained from DGLAP fits to the 1994 H1 measurement of $x_{I\!P} \cdot F_2^{D(3)}(Q^2, x_{I\!P}, \beta)$, as a function of z, the pomeron momentum fraction carried by the parton entering the hard interaction. The curves represent the gluon contributions for the best fit ("fit 3", dashed-dotted curves) and for the case of a flat gluon contribution at the starting scale ("fit 2", dashed curves); the lower curves correspond to the light quark contributions.

It is important to note however that the use of the DGLAP evolution equation may not be valid over the whole β range. It has been stressed (see e.g. [38,47]) that three different contributions, with different Q^2 evolutions, may dominate different β regions: $q\bar{q}g$ at small β (large M_X masses); transversely polarised $q\bar{q}$ systems in the central β region ($0.2 \lesssim \beta \lesssim 0.8$); longitudinally polarised $q\bar{q}$ systems for large β values, giving a higher twist contribution. The importance of the longitudinal contribution at high β is supported by the observation of a dominant longitudinal cross section for vector meson production (following eq. 7, low mass vector mesons are generally produced with large β values). A simple DGLAP analysis through the whole kinematic domain can thus be dubious, especially since the superposition of the three contributions could mimic the distributions in Fig. 12 (see Fig. 15, taken from [47]). However, it should be noted that the H1 conclusions are basically unaffected if the fit domain is restricted to $\beta < 0.65$.[13]

[13]Since the Rio Workshop, a model – of which the general lines are based on an analysis of jet diffractive production [48] – has been proposed to describe inclusive diffraction [49]. This model provides a

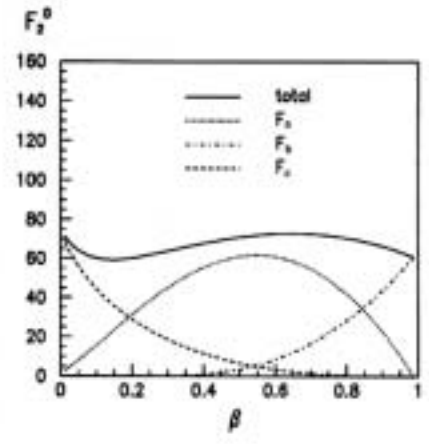

FIG. 15. Shape of the three contributions expected to contribute to inclusive DIS diffraction: $q\bar{q}g$ Fock states at small β values (dashed line, F_c); transversely polarised $q\bar{q}$ states at medium β values (dotted line, F_a); longitudinally polarised $q\bar{q}g$ states at large β, with a higher twist behaviour (dash-dotted line, F_b).

D. Monte-Carlo Programs: RAPGAP and LEPTO

Monte-Carlo programs provide basic tools for experimental studies: they are used to correct the raw data for acceptance, efficiency and smearing effects, and modelise theoretical predictions in a form directly comparable to the measurements.

In the field of diffraction, two main Monte-Carlo simulations are available for DIS interactions: the RAPGAP and LEPTO programs.

The RAPGAP program [52], based on a factorisable pomeron flux, uses parton distribution functions in the pomeron evolved following the DGLAP equations. At the starting scale, the distributions can be modelised as a $q\bar{q}$ system, following the results of the fits to the $F_2^{D(3)}$ scaling violations, or any other form. The photon interaction thus takes place directly on a quark in the pomeron (Fig. 11b), or via boson-gluon fusion (Fig. 11d). In both cases, a "pomeron remnant" is present (a quark in the first case, a gluon in the second case). Higher order contributions (e.g. the QCD-Compton diagram), hadronisation processes and QED radiation are incorporated.

The LEPTO 5.1 Monte Carlo program [43] is the implementation of the concept of SCI in the framework of the Lund model. LRG event are produced as for "normal" deep-inelastic scattering, using standard parameterisations of the parton densities in the proton, but parton reconnection by soft gluons, with pure colour exchange and no kinematics modification, generates neutral partonic systems. Compared to "normal" DIS interactions, the only adjustable parameter in LEPTO 5.1 is the amount of soft colour interactions, and the program is thus highly constrained.

For photoproduction, the POMPYT program [53] is a diffractive-specific extension to PYTHIA, containing both direct and resolved photon interactions.

---

parameterisation of the three major contributions (leading twist longitudinal and transverse cross sections, and higher twist longitudinal contribution). This model has been compared to the ZEUS [29] and H1 [26] measurements. The two experiments give different numerical results for the fitted parameters, which can be traced to the differences in the measurements visible in Fig. 8. More precise measurements and a better understanding of systematic uncertainties are thus necessary before a detailed interpretation of the fit results is possible. However, a common feature for both experiments is the need for a significant contribution of the higher twist longitudinal cross section at high β. Two models based on BFKL dynamics [50,51] were also compared to the H1 measurement [26].

IV. INCLUSIVE AND SEMI-INCLUSIVE FINAL STATE STUDIES

The H1 and ZEUS collaborations have performed numerous studies of the features of inclusive and semi-inclusive diffractive final states (the photon dissociation system X). The most inclusive studies concern the event shape (thrust and sphericity), charged particle multiplicities (total multiplicity, rapidity distributions, forward-backward correlations), energy flow and single particle properties (x_F distributions, transverse momentum spectra, the "sea-gull" plot). Semi-inclusive studies have been performed of jet and of charm production. These measurements are reviewed in detail in separate contributions to this Conference [54–56], and only motivations and general features of the analyses will be presented in this introduction.

Although definite theoretical predictions are presently lacking, especially for the overall features of diffractive final states, an experimental study of the data has provided useful informations on the structure of diffraction. This information was gained both through model independent comparisons of the characteristics of diffractive events with those of other processes, and through the confrontation to the data of Monte Carlo predictions. In particular, RAPGAP calculations are used to test the sensitivity of the final state features to the input parton distributions, as obtained from DGLAP fits to the total inclusive diffractive cross section (see section III C). The pomeron modelisation as a $q\bar{q}$ system, although inconsistent with the fits to the structure function measurements, is often used for comparison.

A. Expected Qualitative Features of Diffractive Final States

It is useful to contrast, as a first order approach, the implications for the hadronic final state of two basic underlying parton topologies: two- and three-body final states, as illustrated in Fig. 11.

The left-hand side diagrams (a,c) of Fig. 11 correspond to the photon fluctuation picture (the strong interaction between the proton and the photon hadronic fluctuations, modelised in the simplest case as two-gluon exchange, is illustrated by one of the relevant diagrams). The right-hand side diagrams (b,d) illustrate the pomeron structure function approach.

The upper two figures correspond to two-body final states: the $q\bar{q}$ Fock state of the photon (a), and the $q\bar{q}$ contribution to the pomeron (b).

The lower two figures correspond to three-body final states. The left-hand side diagram (c) corresponds to the $q\bar{q}g$ Fock state of the photon. In the right-hand side picture (d), the pomeron is a two-gluon object, which interacts with the photon through boson-gluon fusion (BGF).

The characteristic feature of the two-body case is a jetty structure of the X system, aligned with the photon-pomeron direction. Photon fluctuations into $q\bar{q}$ pairs with large transverse momenta (Fig. 11a) have small interaction cross section with the proton because this topology corresponds, through the uncertainty principle, to a small transverse distance between the quarks, which thus screen each other and form a nearly colour neutral system when seen from the proton. This screening effect damps the large p_T contributions, and favours an aligned jet topology. Note that, in the structure function approach for a $q\bar{q}$ pomeron (Fig. 11b), QCD-Compton emission can induce an increase of the final state sphericity and the generation of large transverse momenta, but this process is suppressed by an additional power of α_s.

Three-body final states are characterised by a dominant effective colour octet-octet interaction [47]. In the $q\bar{q}g$ Fock state picture of Fig. 11c, both the fast $q\bar{q}$ system and the soft gluon are colour octets. The topology is similar for Fig. 11d, with a forward going $q\bar{q}$ system and a pomeron remnant. The octet-octet interaction between the forward and backward regions in Fig. 11c,d leads to an increased activity (energy flow, particle multiplicity) in the central region, compared to the triplet-triplet case of the two body $q\bar{q}$ final states of Fig. 11a,b, expected to be close to the e^+e^- case.

B. Inclusive Final States

The event shape of diffractive events has been studied by H1 [57] and ZEUS [58,59]. The X system is mostly aligned with the photon-pomeron direction. However, a significant fraction of the events have a large P_t, the component of the thrust jet momentum transverse to the photon direction in the X system rest frame (see Fig. 16a). In addition, for the same kinematic domain, the average thrust value is smaller than for e^+e^- interactions, and the sphericity is larger (see Fig. 16b).[14] These features suggest that, compared to a basic aligned jet two-parton topology, which is expected to be close to the topology observed in e^+e^- interactions, higher parton multiplicities are also at work in diffraction. This is confirmed by the comparison with RAPGAP predictions: thrust values for a purely $q\bar{q}$ pomeron are significantly higher than observed, whereas the gross features of the data are reasonably reproduced by a gluon dominated pomeron, following the parton distributions obtained from the inclusive cross section measurement.

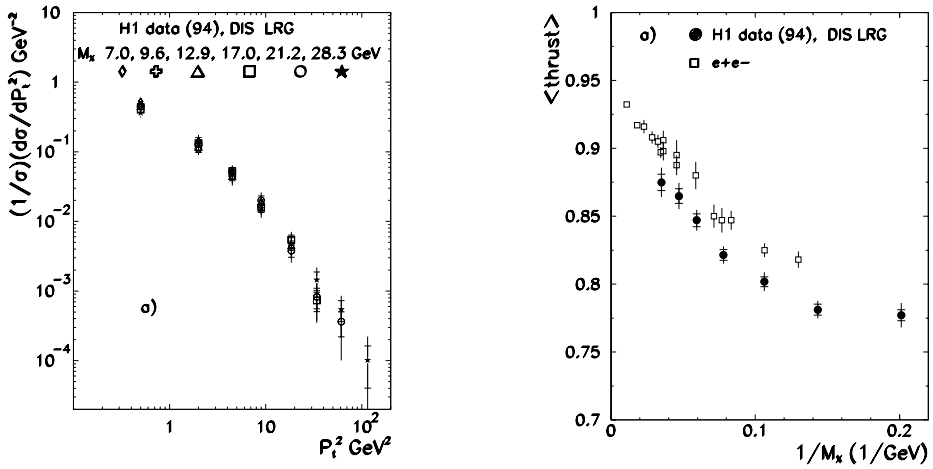

FIG. 16. H1 measurement with the 1994 data of a) the normalised thrust jet P_t^2 distributions for six M_X intervals; b) the average thrust, as a function of $1/M_X$ (solid circles); the open squares are for e^+e^- data, with $s(e^+e^-) = M_X^2$.

Both HERA experiments have also measured the momentum distributions of charged particles in the forward (photon) and backward (pomeron) hemispheres of diffractive events [59,60]. These spectra have been compared by H1 to those obtained in fixed target non-diffractive DIS lepton-proton interactions in the same kinematic range ($W^{DIS} \simeq M_X^{LRG}$). Whereas in DIS a strong asymmetry is observed between the photon hemisphere and the proton remnant region, characterised by a reduced particle emission, the momentum spectra are similar for both hemispheres of LRG events (see Fig. 17, left [60]), and they are softer than for DIS. The distribution of the average transverse momentum squared (with respect to the photon direction in the X system rest frame) as a function of x_F ("sea-gull" plots – Fig. 17, right), show that charged particles in LRG events have larger transverse momentum than in DIS events. These features point towards a significant role of photon fluctuation topologies of the type $q\bar{q}g$ or, equivalently, towards a gluonic pomeron.

[14] Although the LPS ZEUS data [59] are compatible with the e^+e^- results, they are affected by large errors, and are also compatible with the LRG results of H1 [57] and ZEUS [58].

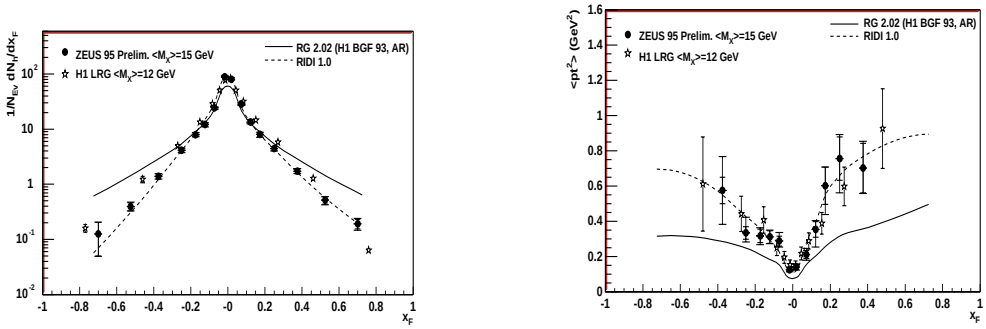

FIG. 17. Measurements with the ZEUS LPS (closed circles) and by H1 (stars) of the scaled longitudinal momentum x_F (left) and of the average transverse momentum squared (with respect to the photon-pomeron axis) as a function of x_F, for charged particles (right). The curves are model predictions.

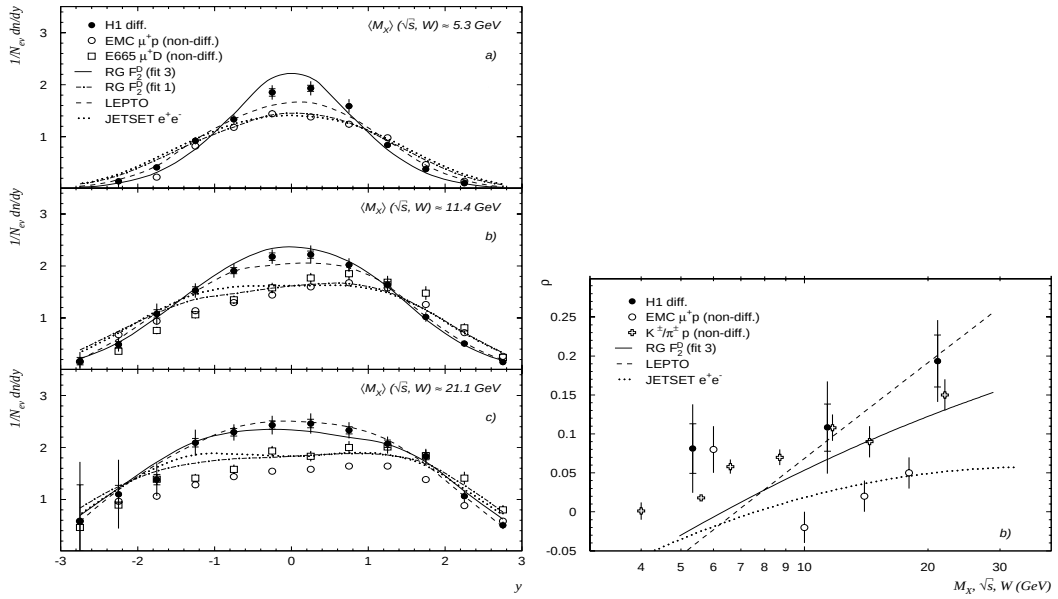

FIG. 18. Left: charged particle multiplicity distribution of DIS LRG events, measured by H1 for three intervals of M_X, compared to non-diffractive lepton−proton data and to e^+e^- interactions, represented by the JETSET calculation. Right: correlations between the backward and forward hemispheres for H1 LRG events, compared to non-diffractive lepton−proton and meson−proton data and to e^+e^- interactions, represented by the JETSET calculation. The curves are predictions of several Monte Carlo models: RAPGAP with the parton distributions extracted from a DGLAP fit to the inclusive diffractive cross section ("fit 3") or with quarks only at the starting scale ("fit 1"), LEPTO, JETSET.

Multiplicity [61] and energy flow [60] studies reinforce these conclusions. The central charged particle multiplicity for diffractive events is significantly higher than for e^+e^- events (see Fig. 18, left), which is attributed to stronger parton radiation in the effective octet-octet structure of

diffraction than for the triplet-triplet interactions of e^+e^- data. The role of gluons is confirmed by the comparison of the data with predictions of the RAPGAP model: the central activity, both for particle multiplicity and energy flow, is well described by the RAPGAP Monte Carlo when using the parton distributions as obtained from the DGLAP fit to the inclusive cross section measurement, whereas the prediction is significantly too low for a hypothetic $q\bar{q}$ pomeron. Finally, the correlations in the multiplicity distributions between the backward and forward hemispheres in diffractive DIS (Fig. 18, right) are stronger than for e^+e^- or non-diffractive lepton hadron interactions, which correspond to triplet-triplet topologies. In contrast, they are of comparable strength to those in soft hadron interactions, where the strong correlations are attributed to the number of overlapping strings in phase space.

It must be noted that most features of the diffractive final states are not only well reproduced by a gluon dominated pomeron as implemented in RAPGAP, but also by the LEPTO SCI model. This is consistent with the major role attributed to gluons in diffraction, since the low x parton distribution functions, with an important gluon contribution, are input to the LEPTO model.

C. Jet and Charm Production

The studies of inclusive properties of the diffractive final state are complemented by semi-inclusive studies of the characteristics of jet and charm production in diffraction.

The particular interest of these processes is in the presence of a well defined hard scale (jet p_t or charm mass), which provides an access to perturbative QCD calculations. Unfortunately, the cross section for jet production is small, and stringent experimental selection procedures have to be imposed to select open charm events. The full potential of these processes for understanding hard diffraction has thus not been exploited yet.

Jets with transverse momenta larger than 5 (H1) or 6 GeV (ZEUS), defined with respect to the photon direction in the rest frame of the system X, have been studied in photoproduction both by H1 [62] and ZEUS [63], and in DIS by H1 [62].

In photoproduction, the distribution of the x_γ variable, which describes the fraction of the photon momentum entering the hard interaction, requires the presence of both a direct ($x_\gamma \simeq 1$) and a resolved ($x_\gamma < 1$) contribution (see Fig. 19, left).

Both for photoproduction and DIS jet production, a sizeable contribution is observed of events where a large fraction z of the pomeron momentum enters the hard interaction; however, the cross section increases as z decreases, suggesting the presence of pomeron remnants (see Fig. 19b, right). This supports the hypothesis of a small jet cross section for a $q\bar{q}$ Fock state, due to screening effects (see section IV A), as demonstrated by the fact that the predictions of a relevant model [64] and of the RAPGAP Monte Carlo with a $q\bar{q}$ pomeron at the starting scale are significantly too small. The bulk of the data is thus explained by $q\bar{q}g$ states, as expected both in perturbative QCD calculations (see e.g. [38,47]) and in a semi-classical approach of soft colour interactions [65].

The results of both experiments support models where the partonic structure of the pomeron is dominated by hard gluons. This is shown by ZEUS using a simultaneous fit of the inclusive diffractive DIS cross section and of the jet production cross section, and by H1 by implementing in the RAPGAP calculation the parton densities obtained from the fits to the scaling violations in inclusive DIS. H1 observes that parton distributions in which the pomeron gluon structure is relatively flat ("fit 2" in [25]) describe the data better than those in which the gluon distribution is peaked at large z ("fit 3"). In resolved photoproduction, a possible underlying interaction between the proton and the photon remnant can be parameterised as a "survival probability" [66]. The best description of the combined DIS and photoproduction data is obtained when a rapidity gap survival probability of 0.6 is applied to the "flat" gluon distribution, but the measurements are affected by large uncertainties.

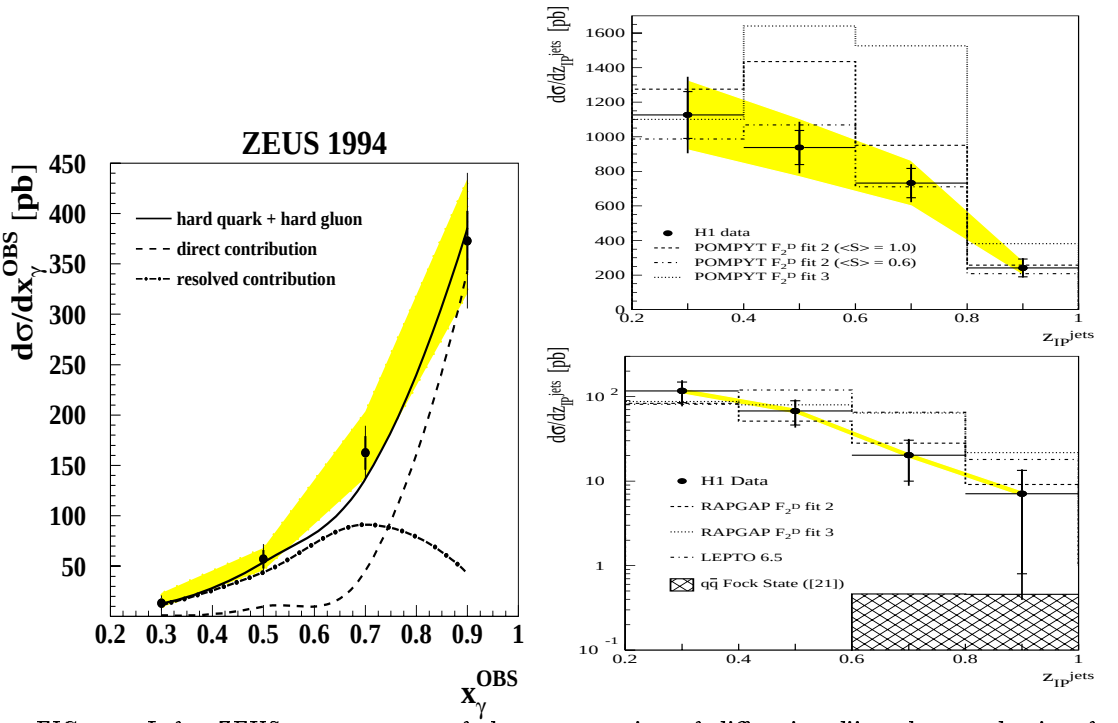

FIG. 19. Left: ZEUS measurement of the cross section of diffractive dijet photoproduction for $E_T^{jet} > 6$ GeV and $-1.5 < \eta^{jet} < 1$, as a function of x_γ, the fraction of the photon momentum entering the hard interaction; the shaded area represents a systematic uncertainty due to the absolute energy scale of the jets; the curves represent the resolved (dot-dashed line), the direct (dashed line) and the resolved + direct contributions, based on the pomeron parton distribution parameterised as hard quarks and hard gluons, in a joint QCD fit of the inclusive DIS diffractive cross section and the dijet diffractive photoproduction. Right: H1 measurements of the cross section of diffractive dijet photoproduction (top) and of DIS production (bottom) for $p_T^{jet} > 5$ GeV and $-1 < \eta^{jet} < 2$, as a function of z, the fraction of the pomeron momentum entering the hard interaction; the shaded bands show the overall normalisation uncertainties; the data are compared to the predictions of the POMPYT (photoproduction) and RAPGAP (DIS) Monte Carlo models with parton densities dominated by a "flat" ("fit 2") or "peaked" ("fit 3") gluon distribution at the starting scale; in the photoproduction case, the POMPYT prediction for the "flat" distribution is also shown for a survival probability of 0.6; in the DIS case, the prediction of a $q\bar{q}$ Fock state calculation is shown as well.

Diffractive exchange is also manifest in a class of events containing jets, and characterised by the absence of hadronic activity between the jets. In photoproduction, both ZEUS and H1 have observed a signal for such events, in excess over the exponential fall-off expected from "usual" colour exchange and hadronisation properties (see Fig. 20, left). This signal is attributed to the exchange between the hard partons producing the jets of a coulour-singlet object, presumably the pomeron.

Following a suggestion to relax the requirement of observing the two jets in the main detector [69], the H1 collaboration has selected photoproduction events characterised by the presence of a gap in rapidity of at least 1.5 units between two systems, X and Y, of masses $M_X, M_Y \ll W$, with $|t| = p_{tX}^2 > 20$ GeV^2 [70]. In the selected kinematics range, a significant excess of events is observed above the expectation for standard photoproduction processes (see Fig. 20, right). The measurement is performed differentially in $x_{I\!P}$, and allows direct comparison with predictions based on perturbative QCD calculations [69]: although the absolute nor;alisation is uncertain, the slope is well described, in contrast with the case of "standard" Monte Carlo simulations.

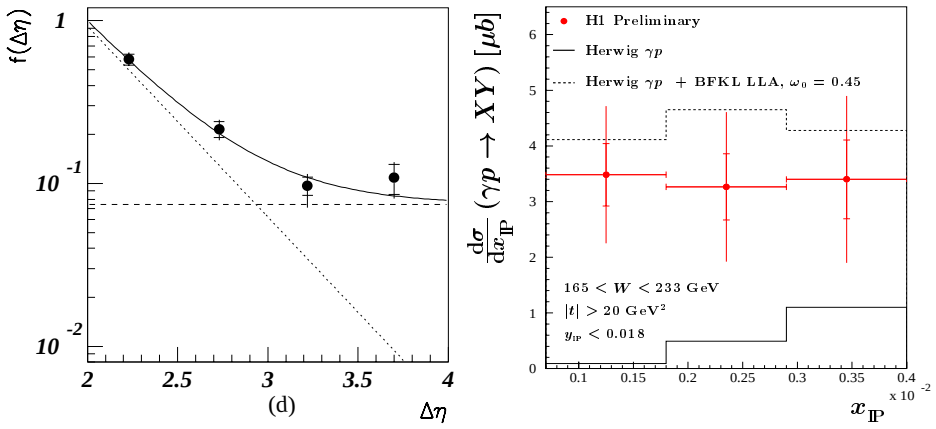

FIG. 20. Left: ZEUS measurement of the fraction of dijet photoproduction events separated by the interval $\Delta\eta$ in rapidity, with no hadronic activity between the jets, as a function of $\Delta\eta$; the distribution is fitted as the sum of an exponentially falling contribution (dotted line), attributed to events with "usual" colour exchange properties, and of a constant contribution (dashed line), attributed to colour-singlet exchange between the jets. Right: H1 measurement of the cross section, differential in $x_{I\!P}$, of photoproduction events with four-momentum transfer squared $|t| > 20$ GeV^2; the solid line is the prediction of a standard photoproduction Monte Carlo; the dashed line is the prediction of a model based on perturbative QCD calculations (with well defined slope but uncertain absolute normalisation).

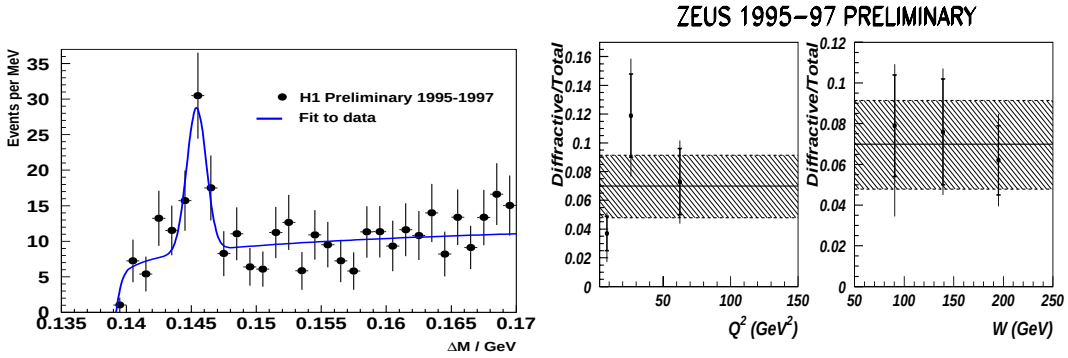

FIG. 21. Left: H1 measurement of the mass difference $\Delta M = M(K^-\pi^+\pi_s^+) - M(K^-\pi^+)$, exhibiting a clear signal for diffractive DIS charm production, of $38 \pm 10 \pm 4$ events. Right: ZEUS measurement of the fraction of diffractively produced $D^{*\pm}$ mesons, as a function of Q^2 and W.

Both experiments have also reported the observation of a signal for diffractive production of open charm in DIS, in the channel $D^{*+} \to D^0\pi_s^+ \to (K^-\pi^+)\pi_s^+$ (and the charge conjugate), where the particle noted π_s^+ is a slow pion [71,72] (see Fig. 21, left). The fraction of diffractively produced $D^{*\pm}$ mesons is measured by ZEUS to be of $7.0 \pm 1.3 \pm 1.7\%$, which is consistent with the fraction of the total DIS cross section attributed to diffraction (see Fig. 21, right). The study of charm production is a promising field to discriminate between several models of diffraction [73]. An important role is assumed to be played by the gluonic content of the pomeron, charm being dominantly produced through the boson-gluon fusion process.

V. EXCLUSIVE VECTOR MESON PRODUCTION

Abundant and very interesting data have been accumulated on exclusive vector meson production, which have only partly been interpreted theoretically.

The most striking feature in this field is the observation of a fast increase with energy of the photoproduction cross section of J/ψ mesons. This increase can be related to the fast increase at low x of the gluon density in the proton, and the understanding of these data is probably the greatest theoretical success so far of perturbative QCD studies in the whole field of diffraction. It is true to say that the low x behaviour of the proton structure function and the energy dependence of J/ψ photoproduction are the two definite evidences of a "hard" behaviour of strong interactions at HERA.

As this rich sample of experimental data has been reviewed in detail in the present Conference [74–76], it will not be discussed in this introduction.

VI. CONCLUSIONS

In the last few years, high energy diffraction has been the subject of great interest, as testified by a large number of publications, both experimental and theoretical, and of specialised workshops, where experimentalists and theorists actively interact.

The large amount of results accumulated at HERA, complemented by data collected at the Tevatron, have renewed the experimental approaches: total cross section measurements have been complemented by studies of the inclusive diffractive final states in the deep-inelastic regime (charged particle distributions and multiplicities, energy flow, event shape), of diffractive jet and charm production, and of exclusive vector meson production. On the theoretical side, in the light of the experimental results, emphasis is placed on the interpretation of diffraction in terms of QCD.

Inclusive interactions of real photons with protons and light vector meson photoproduction are governed, as for hadron–hadron total cross section, by "soft" diffraction, with a mild energy dependence of the cross section. On the other hand, high Q^2 deep-inelastic scattering and J/ψ exclusive production (both by real and virtual photons) reveal a strong energy dependence of the cross section, characteristic of "hard" processes, related to a fast increase of the gluon content in the proton at high energy (low x values). As for total diffractive cross section and light vector meson exclusive electroproduction (with $Q^2 \gtrsim$ a few GeV^2), they present evidence for an interplay between hard and soft diffraction, i.e. between perturbative and non-perturbative QCD features.

The available data are consistent with the interpretation of diffraction as due to the exchange in the t-channel of a gluon dominated object. A DGLAP analysis of scaling violations of the total diffractive cross section, in the form of the $F_2^{D(3)}$ structure function (possibly complemented by a large higher twist contribution at large β), favours the dominance of hard gluons in the pomeron. Assuming factorisation of the cross section into a pomeron flux in the proton and a hard scattering process, the corresponding parton distributions, propagated e.g. through the RAPGAP calculation, give a good description of the inclusive final states and of jet production, whereas the data are inconsistent with a quark dominated pomeron. Seen from the proton rest frame, the data can be interpreted as due mainly to the fluctuation of the photon in a $q\bar{q}g$ Fock state, a $q\bar{q}$ system leading to mutual colour screening of the quarks at large p_T (i.e. for small distances).

It should be noted that many features of the experimental data can also be reproduced by models (specifically the LEPTO calculation) which do not refer to diffraction as a specific process but use the concept of soft colour interactions in the proton, the hard interaction being driven by the gluon dominance in the proton at small x.

More theoretical work is needed to progress in the understanding of diffraction in terms of QCD. In particular, it is important to formulate predictions for the most accessible experimental

characteristics of diffractive events: event shape, energy flow, multiplicity distributions, as well as for jet and charm production.

On the experimental side, a better understanding of the data is necessary in view of resolving the remaining discrepancies between H1 and ZEUS for the total cross section measurement. Major progress is expected from a significant increase of statistics, in particular for the study of hard diffraction: jet and charm production, high Q^2 ($\gtrsim 20$ GeV^2) vector meson production, and particularly high t interactions, for which the present data are very limited. In addition, a measurement of the diffractive longitudinal cross section would be a precious tool to discriminate between models and to specify the domain of applicability of DGLAP evolution equations.

A bright future is open for the study of diffraction and its understanding in terms of QCD.

---

[1] see e.g. P. Collins, *An Introduction to Regge Theory and High Energy Physics*, Cambridge University Press, Cambridge (1977).

[2] A.B. Kaidalov, *Phys. Rep.* **50** (1979) 157.

[3] M.L. Good and W.D. Walker, *Phys. Rev.* **120** (1960) 1857.

[4] G. Alberi and G. Goggi, *Phys. Rep.* **74** (1981) 1.

[5] K. Goulianos, *Phys. Rep.* **101** (1983) 169.

[6] E. Predazzi, *Diffraction: From Origin to Today*, these proc.

[7] A. Donnachie and P.V. Landshoff, *Nucl. Phys.* **B231** (1984) 189; *Nucl. Phys.* **B244** (1984) 322; *Phys. Lett.* **B296** (1992) 227.

[8] J. Cudell, K. Kang, and S. Kim, *Phys. Lett.* **B395** (1997) 311.

[9] WA91 Collab., S. Abatzis et al., *Phys. Lett.* **B324** (1994) 509.

[10] E. Levin, *The Pomeron: Yesterday, Today and Tomorrow*, LAFEX 1994, hep-ph-09503399.

[11] F. Low, *Phys. Rev.* **D12** (1975) 163;
S. Nussinov, *Phys. Rev. Lett.* **34** (1975) 1286.

[12] UA8 Collab., R. Bonino et al., *Phys. Lett.* **B211** (1988) 239;
UA8 Collab., A. Brandt et al., *Phys. Lett.* **B297** (1992) 417.

[13] G. Ingelman and P. Schlein, *Phys. Lett.* **B152** (1985) 256.

[14] H1 Collab., S. Aid et al., *A Measurement and QCD Analysis of the Proton Structure Function $F_2(x,Q^2)$ at HERA*, *Nucl. Phys.* **B470** (1996) 3.

[15] ZEUS Collab., M. Derrick et al., *Measurement of the F_2 Structure Function in Deep Inelastic e^+p Scattering using 1994 Data from the ZEUS Detector at HERA*, *Zeit. Phys.* **C72** (1996) 399.

[16] ZEUS Collab., M. Derrick et al., *Observation of Events with a Large Rapidity Gap in Deep-inelastic Scattering at HERA*, *Phys. Lett.* **B315** (1993) 481.

[17] H1 Collab., T. Ahmed et al., *Deep Inelastic Scattering Events with a Large Rapidity Gap at HERA*, *Nucl. Phys.* **B429** (1994) 477.

[18] H. Kowalski, DIS96 Workshop, Rome 1996, discussion.

[19] A. Donnachie and P.V. Landshoff, *Hard Diffraction at HERA*, Proc. of the HERA Workshop, ed. R.D. Peccei, DESY, Hamburg (1987) 351;
K.H. Streng, *Hard QCD Scattering in Diffractive Reactions at HERA*, ibid. p. 365;
M.G. Ryskin and M. Besançon, *Heavy photon dissociation in deep inelastic scattering*, Proc. of the Workshop "Physics at HERA", ed. W. Buchmüller and G. Ingelman, DESY, Hamburg (1992) 215.

[20] see e.g. A. Brandt, *Hard Diffraction at the Tevatron*, these proc.

[21] H1 Collab., T. Ahmed et al., *First Measurement of the Deep-inelastic Structure of Proton Diffraction*, *Phys. Lett.* **B348** (1995) 681.

[22] H. Kowalski, *Inclusive γ^*p Diffraction*, these proc.

[23] M.F. McDermott and G. Briskin, Proc. of the Workshop on "Future Physics at HERA", ed. G. Ingelman, A. De Roeck and R. Klanner, DESY, Hamburg (1996) 691.

[24] ZEUS Collab., M. Derrick et al., *Measurement of the Diffractive Structure Function in Deep-inelastic Scattering at HERA*, *Zeit. Phys.* **C68** (1995) 569.

[25] H1 Collab., C. Adloff et al., *Inclusive Measurement of Diffractive Deep-inelastic ep Scattering*, *Zeit. Phys.* **C76** (1997) 613.

[26] H1 Collab., *Measurement of the Diffractive Structure Function $F_2^{D(3)}$ at Low and High Q^2 at HERA*, paper 571, subm. to the 29th Int. Conf. on HEP ICHEP98, Vancouver, Canada, 1998.
[27] see e.g. P. Marage, *Aspects of Diffraction Studies*, summary of the discussion session on diffraction, to be publ. in Proc. of the Int. Workshop on Low-x Physics, Madrid, 1997.
[28] ZEUS Collab., M. Derrick et al., *Measurement of the Diffractive Cross Section in Deep Inelastic Scattering*, *Zeit. Phys.* **C70** (1996) 391.
[29] ZEUS Collab., J. Breitweg et al., *Measurement of the Diffractive Cross Section in Deep Inelastic Scattering using ZEUS 1994 Data*, DESY 98-084, subm. to *Eur. Phys. J.*
[30] H. Kowalski, *Inclusive $\gamma^* p$ Diffraction*, these proc.
[31] ZEUS Collab., J.Breitweg et al., *Measurement of the Diffractive Structure Function $F_2^{D(4)}$ at HERA*, *Eur. Phys. J.* **C1** (1998) 61.
[32] ZEUS Collab., J. Breitweg et al., *Measurement of the t Distribution in Diffractive Photoproduction at HERA*, *Eur. Phys. J.* **C2** (1998) 237.
[33] ZEUS Collab., *Measurement of the t distribution in diffractive electron-proton interactions at HERA*, paper 972, subm. to the 29th Int. Conf. on HEP ICHEP98, Vancouver, Canada, 1998.
[34] H1 Collab., S. Aid et al., *Elastic and Inelastic Photoproduction of J/ψ Mesons at HERA*, *Nucl. Phys.* **B472** (1996) 3;
ZEUS Collab., J.Breitweg et al., *Measurement of Elastic J/ψ Photoproduction at HERA*, *Zeit. Phys.* **C75** (1997) 215.
[35] H1 Collab., *Energy Dependence of the Cross Section for the Exclusive Photoproduction of J/ψ Mesons at HERA*, paper 572, subm. to the 29th Int. Conf. on HEP ICHEP98, Vancouver, Canada, 1998.
[36] H1 Collab., C. Adloff et al., *Diffractive Dissociation in Photoproduction at HERA*, *Zeit. Phys.* **C74** (1997) 221.
[37] ZEUS Collab., J. Breitweg et al., *Study of Photon Dissociation in Diffractive Photoproduction at HERA*, *Zeit. Phys.* **C75** (1997) 421.
[38] N.N. Nikolaev and B.G. Zakharov, *Zeit. Phys.* **C53** (1992) 331.
[39] A. Donnachie and P.V. Landshoff, *Phys. Lett.* **B285** (1992) 172;
J.C. Collins, L. Frankfurt and M. Strikman, *Phys. Lett.* **B307** (1993) 161;
A. Berera and J.C. Collins, *Nucl. Phys.* **B474** (1996) 183.
[40] J.C. Collins, *Phys. Rev.* **D57** (1998) 3051.
[41] A. Hebecker, *Nucl. Phys.* **B505** (1997) 349.
[42] W. Buchmüller, *Phys. Lett.* **B353** (1995) 335;
W. Buchmüller, A. Hebecker, *Phys. Lett.* **B355** (1995) 573; *Nucl. Phys.* **B476** (1996) 203.
[43] A. Edin, G. Ingelman and J. Rathsman, *Phys. Lett.* **B366** (1996) 371;
G. Ingelman, A. Edin and J. Rathsman, *Comp. Phys. Comm.* **101** (1997) 108.
[44] J.F. Owens, *Phys. Rev.* **D30** (1984) 943.
[45] ZEUS Collab., M. Derrick et al., *Diffractive hard photoproduction at HERA and evidence for the gluon content of the pomeron*, *Phys. Lett.* **B356** (1995) 129;
ZEUS Collab., J. Breitweg et al., *Diffractive Dijet Cross Sections in Photoproduction at HERA*, DESY 98-045, subm. to *Eur. Phys. J.*
[46] L. Alvero, J.C. Collins, J. Terron and J.J. Whitmore, *Diffractive Production of Jets and Weak Bosons and Tests of Hard-Scattering Factorization*, hep-ph/9805268;
J. Whitmore, *Extracting the Pomeron Structure Function from HERA Data*, these proc.
[47] M. Wüsthoff, *Phys. Rev.* **D56** (1997) 4311.
[48] J. Bartels, *Jet Production in Diffractive Dissociation*, these proc.
[49] J. Bartels, J. Ellis, H. Kowalski and M. Wüsthoff, *An Analysis of Diffraction in Deep-Inelastic Scattering*, hep-ph/9803497.
[50] A.H. Mueller and B. Patel, *Nucl. Phys.* **B425** (1994) 471;
H. Navelet, R. Peschanski, C. Royon and S. Wallon, *Phys. Lett.* **B385** (1996) 357;
A. Bialas, R. Peschanski and C. Royon, *Phys. Rev.* **D57** (1998) 6899.
[51] M. Bertini et al., *Phys. Lett.* **B422** (1998) 238;
M. Genovese and N.N. Nikolaev, *J. Exp. Theor. Phys.* **81** (1995) 633.
[52] H. Jung, *Comp. Phys. Comm.* **86** (1995) 147.
[53] P. Bruni and G. Ingelman, Proc. of the Int. Europhys. Conf. on HEP, Marseilles, France, 1993.
[54] A. Valkarova, *Hadronic Final States in $\gamma^* p$ Diffraction*, these proc.
[55] J. Zsembery, *Dijet in $\gamma^* p$ Diffraction*, these proc.

[56] B. Cox, *Rapidity Gaps Between Jets in γp Interactions*, these proc.
[57] H1 Collab., C. Adloff et al., *Thrust Jet Analysis of Deep-Inelastic Large-Rapidity-Gap Events*, *Eur. Phys. J.* **C1** (1998) 495.
[58] ZEUS Collab., J.Breitweg et al., *Event Shape Analysis of Deep Inelastic Scattering Events with a Large Rapidity Gap at HERA*, *Phys. Lett.* **B421** (1998) 368.
[59] ZEUS Collab., *Properties of hadronic final states in diffractive deep inelastic ep scattering at HERA*, paper 787, subm. to the 29th Int. Conf. on HEP ICHEP98, Vancouver, Canada, 1998.
[60] H1 Collab., C. Adloff et al., *Hadron Production in Diffractive Deep Inelastic Scattering*, *Phys. Lett.* **B428** (1998) 206.
[61] H1 Collab., C. Adloff et al. *Multiplicity Structure of Hadronic Final States in Diffractive Deep-Inelastic Scattering at HERA*, DESY-98-044, subm. to *Eur. Phys. J.*
[62] H1 Collab., C. Adloff et al. *Diffractive Dijet Production at HERA*, DESY-98-092, subm. to *Eur. Phys. J.*
[63] ZEUS Collab., J.Breitweg et al. *Diffractive Dijet Cross Sections in Photoproduction at HERA*, DESY 98-045,
[64] J. Bartels, H. Lotter and M. Wüsthoff, *Phys. Lett.* **B379** (1996) 239;
J. Bartels, C. Ewerz, H. Lotter and M. Wüsthoff, *Phys. Lett.* **B386** (1996) 389.
[65] W. Buchmüller, M.F. McDermott and A. Hebecker, *Phys. Lett.* **B410** (1997) 304.
[66] J. Bjorken, *Phys. Rev.* **D47** (1993) 101;
E. Gostman, E. Levin and U. Maor, *Phys. Lett.* **B309** (1993) 199.
[67] ZEUS Collab., M. Derrick et al., *Rapidity Gaps between Jets in Photoproduction at HERA*, *Phys. Lett.* **B369** (1996) 55.
[68] H1 Collab., *Rapidity Gaps between Jets in Photoproduction at HERA*, paper 380, subm. to the Int. Europhys. Conf. on HEP, Jerusalem, Israel, 1997.
[69] B.E. Cox and J.R. Forshaw, *Double Diffraction Dissociation at Large t*, hep-ph/9805206.
[70] H1 Collab., *Double Diffraction Dissociation at large $|t|$*, paper 570, subm. to the 29th Int. Conf. on HEP ICHEP98, Vancouver, Canada, 1998.
[71] H1 Collab., *Diffractive Charmonium Production in Deep Inelastic Scattering at HERA*, paper 572, subm. to the 29th Int. Conf. on HEP ICHEP98, Vancouver, Canada, 1998.
[72] ZEUS Collab., *Open Charm Production in Diffractive Deep Inelastic Scattering at HERA*, paper 785, subm. to the 29th Int. Conf. on HEP ICHEP98, Vancouver, Canada, 1998.
[73] M. Genovese et al., *Phys. Lett.* **B378** (1996) 347;
W. Buchmüller, A. Hebecker and M.F. McDermott, *Phys. Lett.* **B404** (1997) 353;
H. Lotter, *Phys. Lett.* **B406** (1997) 171;
E.M. Levin et al., *Zeit. Phys.* **C74** (1997) 671;
M. Diehl, *Eur. Phys. J.* **C1** (1998) 293;
L.P.A. Haakman et al, *Eur. Phys. J.* **C1** (1998) 547.
[74] J. Whitmore, *Light Vector Meson Production at HERA*, these proc.
[75] J. Crittenden, *Scale Issues in High-Energy Diffractive Vector-Meson Production*, these proc.
[76] L. West, *Diffractive Heavy Flavour Production at HERA*, these proc.